Environ. Sci. Technol. **2002**, *36,* 1093−1101

Evaluating Remedial Alternatives for an Acid Mine Drainage Stream: Application of a Reactive Transport Model

ROBERT L. RUNKEL*

U.S. Geological Survey, MS 415, Denver Federal Center, Denver, Colorado 80225

BRIANT A. KIMBALL

U.S. Geological Survey, 2329 W Orton Circle, West Valley City, Utah 84119

A reactive transport model based on one-dimensional transport and equilibrium chemistry is applied to synoptic data from an acid mine drainage stream. Model inputs include streamflow estimates based on tracer dilution, inflow chemistry based on synoptic sampling, and equilibrium constants describing acid/base, complexation, precipitation/dissolution, and sorption reactions. The dominant features of observed spatial profiles in pH and metal concentration are reproduced along the 3.5-km study reach by simulating the precipitation of Fe(III) and Al solid phases and the sorption of Cu, As, and Pb onto freshly precipitated iron(III) oxides. Given this quantitative description of existing conditions, additional simulations are conducted to estimate the streamwater quality that could result from two hypothetical remediation plans. Both remediation plans involve the addition of $CaCO_3$ to raise the pH of a small, acidic inflow from ∼2.4 to ∼7.0. This pH increase results in a reduced metal load that is routed downstream by the reactive transport model, thereby providing an estimate of post-remediation water quality. The first remediation plan assumes a closed system wherein inflow Fe(II) is not oxidized by the treatment system; under the second remediation plan, an open system is assumed, and Fe(II) is oxidized within the treatment system. Both plans increase instream pH and substantially reduce total and dissolved concentrations of Al, As, Cu, and Fe(II+III) at the terminus of the study reach. Dissolved Pb concentrations are reduced by ∼18% under the first remediation plan due to sorption onto iron(III) oxides within the treatment system and stream channel. In contrast, iron(III) oxides are limiting under the second remediation plan, and removal of dissolved Pb occurs primarily within the treatment system. This limitation results in an increase in dissolved Pb concentrations over existing conditions as additional downstream sources of Pb are not attenuated by sorption.

Introduction

Streams and rivers affected by acid mine drainage are complex systems in which hydrologic and geochemical processes interact to determine the fate and transport of trace metals. Study of trace metal behavior in these systems is further complicated by spatial and temporal variability in the relevant processes. A standard approach to address process interaction and variability is to employ solute transport models that include a description of hydrologic transport (e.g., ref *1*) and a geochemical submodel (*2*−*8*). Many of these models characterize geochemical reactions using first-order rate constants that do not explicitly consider the effects of pH, ionic strength, and solute interaction. In an effort to more rigorously describe trace metal geochemistry, a reactive transport model known as OTEQ has been developed by coupling hydrologic transport with a chemical equilibrium submodel (*9*, *10*). Advantages of this coupled approach include the ability to consider solute interactions (e.g., the effect of precipitation reactions on pH), the pH dependence of sorption, and the linkage between the precipitation of iron oxides and sorption (*10*).

Applications of OTEQ to date have focused on the analysis of geochemistry and transport during pH-modification experiments (*10*−*12*). These experiments represent dynamic conditions that mimic events such as episodic acidification, blowouts, and accidental spills (e.g., ref *13*). Analyses of these experiments have provided quantitative descriptions of trace metal behavior as a pH pulse propagates its way through the hydrologic system. Another application of interest is quantification of the processes that determine the steady-state profile of trace metals and pH. This application is especially important when considering the potential effects of remediation on streamwater quality. Model application to steady-state data provides a means to describe the processes controlling metal concentrations as well as the sources of metals and acidity. Given this quantitative description of existing conditions, additional simulations may be conducted to estimate streamwater quality that might be achieved under various remediation plans.

Although considerable progress has been made in regard to the treatment of acid mine drainage (*14*−*23*), relatively little attention has been paid to the effects of treatment on downstream water quality. The purpose of this paper is to demonstrate how OTEQ may be used to evaluate remedial alternatives for streams affected by acid mine drainage. This demonstration is based on data from Mineral Creek, an acid mine drainage stream in southwestern Colorado. OTEQ is first used to reproduce the spatial profiles of metals and pH observed in Mineral Creek during September 1999. This description of existing conditions provides a calibrated model that is subsequently used to evaluate two hypothetical remediation plans. Simulations of remedial actions are compared with existing conditions to evaluate the potential improvements in streamwater quality.

Methods

Study Location. The San Juan Mountains of southwestern Colorado contain numerous headwater streams that are contaminated by acid mine drainage. Mineral Creek is one of several streams in the San Juan Mountains that have been studied by the U.S. Geological Survey as part of the Abandoned Mine Lands Initiative (*24*). Mineral Creek originates at the top of Red Mountain Pass north of Silverton, CO (Figure 1), and flows ∼15 km before entering the Animas River. The subject of this paper is the upper 3.5 km of Mineral Creek, a free-flowing section of the stream that is constrained by a steep canyon (stream slope ∼73 m/km). Stream depth during low-flow periods is generally <0.5 m, and stream width ranges from 1 to 3 m. Numerous inflows along the study reach introduce metals and acidic waters. The metal-rich,

* Corresponding author phone: (303)236-4882; fax: (303)236-4912; e-mail: runkel@usgs.gov.

10.1021/es0109794
Published on Web 01/19/2002

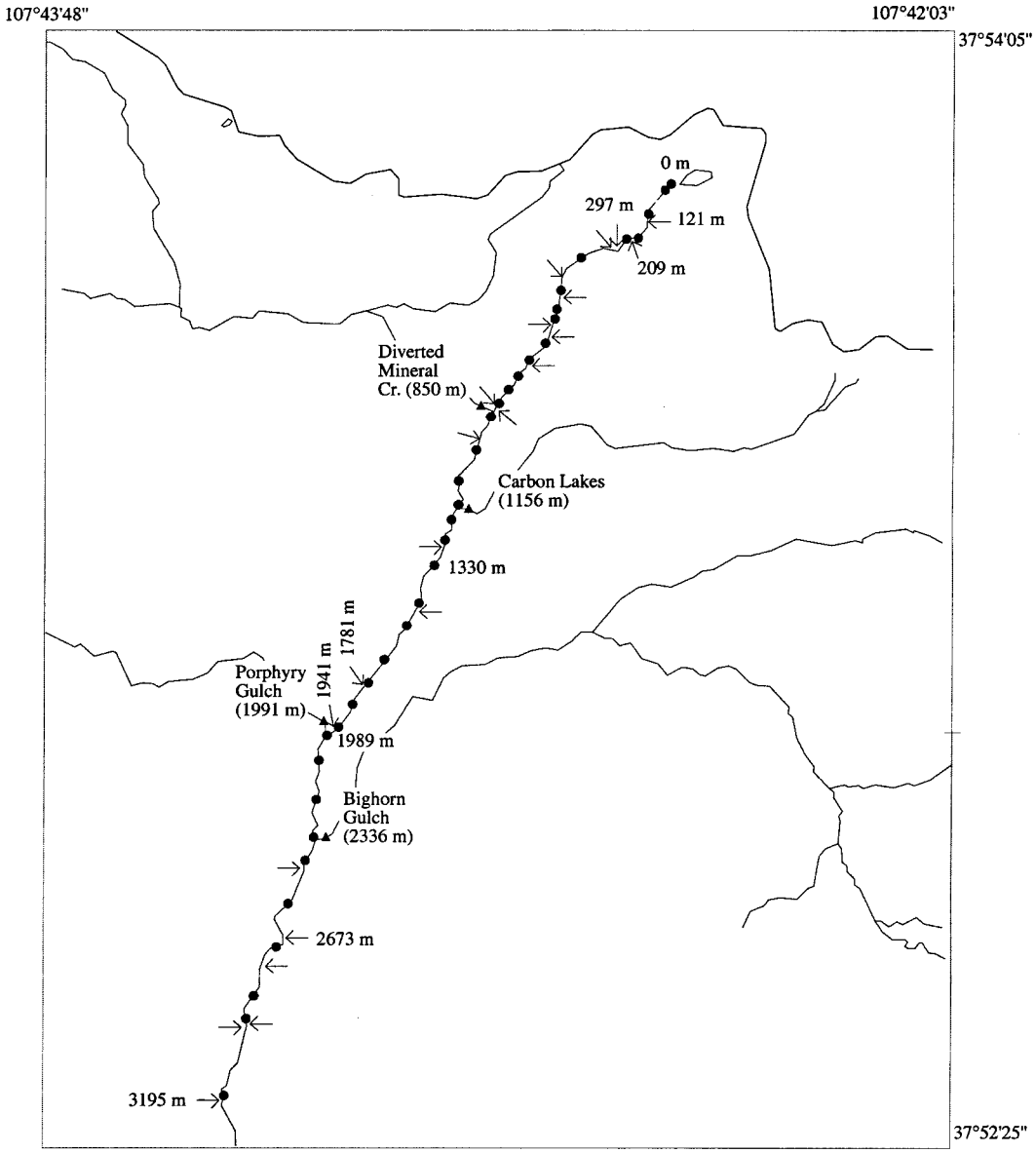

FIGURE 1. Map of Mineral Creek including instream (circles) and inflow sampling (arrows and triangles) locations.

acidic inflows drain alteration zones of the Silverton Volcanics, which are porphyritic andesitic flows, containing 15−25% phenocrysts of plagioclase and augite. In the study area, there is local alteration to a quartz−sericite−pyrite assemblage, which contains complete replacement of plagioclase and potassium feldspar by fine-grained quartz, illite (sericite), and 10−20% finely disseminated and fracture-filling pyrite (D. Bove, U.S. Geological Survey, written communication). Inflows consist of both mine drainage and natural sources draining mineralized areas. Elevated concentrations of iron, aluminum, copper, and zinc are observed, and pH ranges from 2.5 to 6.0 throughout the study reach. Under these conditions, precipitated hydrous iron oxides coat the streambed, and the stream is virtually devoid of typical montane aquatic life.

Tracer Injection and Synoptic Sampling. Quantification of metal sources and constituent loads requires estimates of both streamflow and solute concentration. An approach used in acid mine drainage streams is to combine the tracer-dilution method with synoptic sampling (*4*, *25*, *26*). The tracer-dilution method provides estimates of streamflow (*27*), and synoptic sampling provides a description of instream and inflow chemistry. On September 16, 1999, a continuous injection of a ~0.7 M LiBr solution was initiated at the upstream end of the study reach (0 m, Figure 1). Synoptic samples were collected at 38 stream sites and 26 inflow locations (Figure 1) on the following day after instream Br concentrations had reached a steady-state plateau. Sampled inflows ranged from small trickles of water off rock faces to well-defined tributaries such as Big Horn Gulch. Photographs of several sampling locations are available (http://co.water.usgs.gov/toxics).

Samples were collected in 1.8-L HPDE bottles and transported to a central processing area in black plastic bags to avoid exposure to direct sunlight. Upon arrival at the processing area, 125-mL aliquots were prepared for cation and anion analyses. On-site processing included filtration, pH measurement, and preservation of samples for iron speciation. Filtration was completed using tangential flow units equipped with 10 000-Da molecular mass membranes. Aliquots for iron speciation were placed in amber bottles and preserved with concentrated HCl to fix the Fe(II)/Fe(III) ratio in filtered samples (*28*). Aliquots for cation analysis were acidified to pH < 2.0 with ultrapure HNO_3. Total recoverable and dissolved cation concentrations were determined from unfiltered and filtered samples, respectively,

TABLE 1. Model Reaches Including Streamflow, Inflow Locations, and Fe(II) Percentages

reach and distance (m)	streamflow (L/s) top of reach	streamflow (L/s) w/i reach increase	locations of observed inflows (m)[a]	Fe(II) %
1: 0−120	1.70	0.15	none	90
2: 120−176	1.85	0.07	**121**	90
3: 176−226	1.93	4.22	**209**	60
4: 226−376	6.15	0.71	297, **307**	60
5: 376−432	6.86	13.78	**410**	60
6: 432−656	20.63	1.33	**435**, 518, 563	70
7:-656−826	21.96	2.41	**662**	70
8: 826−888	24.38	68.82	827, 836, **850-diverted mineral**	78
9: 888−1151	93.2	0	940	78
10: 1151−1194	93.2	14.19	**1156-carbon lakes**	78
11: 1194−1244	107.39	0.37	none (**1156**)	78
12: 1244−1330	107.75	1.19	**1254**	78
13: 1330−1530	108.94	1.99	**1472**	78
14: 1530−1831	110.93	2.99	**1781**	78
15: 1831−1989	113.92	1.57	**1941**	78
16: 1989−2041	115.48	56.68	**1991-Porphyry Gulch**	72
17: 2041−2331	172.16	0	none	72
18: 2331−2396	172.16	34.71	*2336-Big Horn Gulch* (**2673**)	72
19: 2396−2980	206.87	12.15	2406, **2673**, 2840	72
20: 2980−3193	219.02	21.21	**3085**, 3086	72
21: 3193−3428	240.24	10.11	**3195**	72
22: 3428−3528	250.34	0	none	72

[a] Inflow used to represent reach inflow chemistry shown in boldface; inflow used to represent reach inflow chemistry during precalibration is shown in italics where different from calibration inflow. Inflow used in calibration is shown in parentheses if it is not within reach boundaries. Reach 1 inflow chemistry set equal to upstream boundary condition.

using inductively coupled argon plasma-atomic emission spectrometry. Dissolved anion concentrations including the Br tracer were determined from filtered, unacidified samples by ion chromatography. Fe(II) and total dissolved iron were determined colorimetrically (*29*). Alkalinity was determined from filtered, unacidified samples.

Estimates of streamflow at 31 stream sites were determined from Br dilution (*27*). Estimation of streamflow at the remaining stream sites was precluded due to an observed increase in Br concentration from 1330 to 1989 m (all distances used herein refer to the distance downstream from the injection site, in meters); a linear increase in flow was therefore assumed from 1330 to 1989 m.

Reactive Transport Modeling. The theoretical framework and governing equations underlying the OTEQ solute transport model are described in detail by Runkel et al. (*9*, *10*). In short, OTEQ is formed by coupling the OTIS solute transport model (*7*) with a chemical equilibrium submodel. The equilibrium submodel is based on MINTEQ (*30*), a model that calculates the distribution of chemical species that exist within a batch reactor at equilibrium. The coupled model considers a variety of processes including advection, dispersion, transient storage, transport and deposition of waterborne solid phases, acid/base reactions, complexation, precipitation/dissolution, and sorption.

Governing equations are formulated in terms of chemical components, where the total component concentration is the sum of all dissolved, precipitated, and sorbed species. In general, precipitated and sorbed species may reside within the water column or on the streambed. For Mineral Creek, mass balance analyses indicate that total recoverable metal concentrations behave in a conservative manner; i.e., any settling of colloidal material is balanced by resuspension. Settling velocities are therefore set to zero so that precipitated and sorbed species remain in the water column and are subject to downstream transport. Total component concentrations are partitioned between dissolved, precipitated, and sorbed phases based on equilibrium submodel calculations for each stream segment.

One set of governing equations is specified for each chemical component. Components used in the Mineral Creek application include Al, Ca, Cd, Cu, CO_3 (total inorganic carbon), Fe(II), Fe(III), H_3AsO_4 (for As(V)), Mg, Mn, Ni, Pb, SO_4, TOTH (total excess hydrogen), and Zn. Precipitation reactions for Al and Fe(III) are defined using microcrystaline gibbsite ($Al(OH)_3$, $\log k = -8.77$) and ferrihydrite ($Fe(OH)_3$) as the solid phases. Sorption of As, Ca, Cd, Cu, Ni, Pb, SO_4, TOTH, and Zn to freshly precipitated iron oxides is modeled using a surface complexation approach and the database of Dzombak and Morel (*10*, *30*, *31*). The mass of sorbent within each stream segment is based on the amount of precipitated Fe(III) within the water column, as determined by the equilibrium submodel. Precipitated Fe(III) on the streambed is assumed to be saturated with respect to sorbed species and is therefore not a sink in the steady-state analysis presented herein. Sorption to aluminum oxides is not considered as water-borne aluminum oxides were not present in portions of the study reach in which sorption is evident (Figure 2 f,k,l). Transfer of mass between Fe(II) and Fe(III) due to microbial oxidation and photoreduction (*32*, *33*) is modeled by specifying the percentage of total dissolved iron (Fe(II) + dissolved Fe(III)) that is Fe(II). This approach is similar to that of Runkel et al. (*12*), except that the percentage is based on total dissolved rather than total recoverable iron concentrations.

Unless noted otherwise, equilibrium constants for acid/base, complexation, precipitation, and sorption reactions are set using default values from the equilibrium submodel (*30*, *31*). Sorption parameters (i.e., specific surface area, sorbent molecular weight, low affinity site density) are set using the best estimates of Dzombak and Morel (*31*). The high affinity site density is set equal to the upper value reported by Dzombak and Morel (*31*), reflecting the high sorptive capacity of freshly precipitated iron oxides (*10*). Equilibrium constants and activity coefficients are adjusted for the effects of temperature (9 °C) and ionic strength (0.003 M) within the equilibrium submodel.

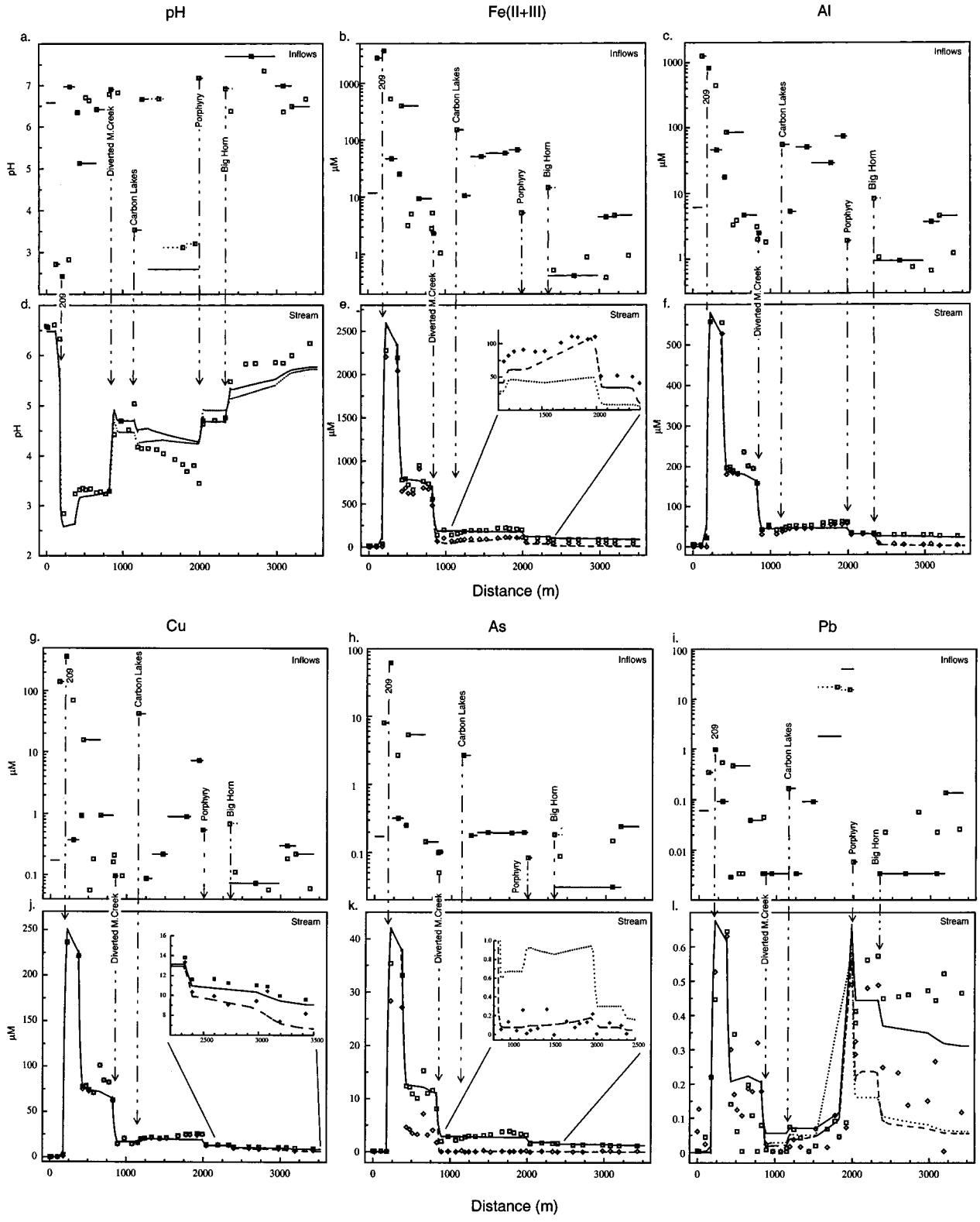

FIGURE 2. Total recoverable inflow concentrations (symbols), model inflow concentrations (solid line), and precalibration model inflow concentrations (dotted line) for pH, Fe(II+III), Al, Cu, As, and Pb (panels a–c and g–i, respectively). Precalibration inflow concentrations are shown only where they differ from model inflow concentrations. Total recoverable (squares), dissolved (diamonds), simulated total recoverable (solid line), simulated dissolved (dashed line), and precalibration dissolved (dotted line) concentrations for instream pH, Fe(II+III), Al, Cu, As, and Pb (panels d–f and j–l, respectively).

Existing Conditions. The first step in the analysis of remediation involves characterization of the hydrologic and geochemical processes that influence existing conditions. Successful modeling of existing conditions requires estimates of streamflow, hydrologic parameters, and chemical data that describe metal loading along the study reach. The 3.5-km study reach was first divided into 22 reaches based on changes in streamflow and water chemistry (Table 1). Streamflow and other hydrologic parameters (velocity, dispersion, transient storage) for each reach were determined

TABLE 2. Inflow Chemistry at 209 m

component	existing conditions (μM)	remediation plan 1 dissolved concn (μM)	remediation plan 1 % decrease [increase]	remediation plan 2 dissolved concn (μM)	remediation plan 2 % decrease [increase]
pH[a]	2.43	7.03		7.03	
Al	823	1.18	99.86	1.18	99.86
As	61.4	0.01	99.98	<0.01	99.99
Cd	1.89	1.88	0.58	1.83	3.12
Cu	364	107	70.54	8.54	97.65
Fe(II)	1834	1834	0.00	0.00	100.00
Fe(III)	1908	0.05	100.00	0.05	100.00
Ni	0.83	0.83	0.19	0.77	6.43
Pb	0.98	0.2	79.11	0.01	99.29
SO_4	9899	9865	0.34	9759	1.41
Zn	841	809	3.75	681	19.03
Ca	1599	14100	[782]	11320	[608]
CO_3	8.21	12508	[152176]	72.55	[783]
$CaCO_3$ added		12500		9721	

[a] In standard units.

based on Br tracer data. Steady-state analyses under the assumption of chemical equilibrium are generally insensitive to the hydrologic parameters, such that specific parameter values are not reported here. Most reaches include one or more observed inflows that were used to set component inflow concentrations. When more than one inflow was available for a given reach, the largest observed inflow was generally used (Table 1). The upstream boundary condition was set using component concentrations of the sample collected at 0 m. Percentages of Fe(II) used to model photoreduction and oxidation were set for each reach based on observed data (Table 1).

Component concentrations at the upstream boundary and within the inflows were set equal to total recoverable concentrations for most components. Two exceptions are TOTH and CO_3, components that were assigned concentrations based on stand-alone MINTEQ computations. In these computations, pH and alkalinity were fixed at observed values, and TOTH and CO_3 were determined from the speciated output. For samples without alkalinity, CO_3 concentrations were based on equilibrium with atmospheric CO_2.

Assignment of inflow chemistry based on the observed inflows and the use of default equilibrium constants results in a generic description of the study reach that has not been calibrated to match observed stream data. This description, known here as "precalibration", reproduces the general features of the observed concentration profiles but is lacking in some respects. Several modifications to the precalibration model were therefore made to improve correspondence between the simulation and observed data. Calibration included the following modifications: (i) the pH of the inflows in reaches 13−15 (1330−1989 m) were decreased from observed values to 2.6; (ii) the ferrihydrite solubility was decreased by changing the equilibrium constant from the default value (−4.89) to −5.29; (iii) the surface complexation constant for sorption of $H_2AsO_4^-$ was changed from the default value (8.67) to 10.17; (iv) the Pb inflow concentrations in reaches 14−15 (1530−1989 m) were adjusted such that the location and magnitude of the observed Pb concentrations were reproduced downstream of 1800 m; and (v) the observed inflow in reach 18 (2331−2396 m), Big Horn Gulch, was replaced by the inflow at 2673 m.

Remediation. Given the calibrated model of existing conditions, two hypothetical remedial plans were considered. Both remediation plans considered the treatment of a small (4.22 L/s) inflow at 209 m with low pH (2.43) and high metal concentrations (Table 2). Treatment consisted of the addition of $CaCO_3$ to increase inflow pH to ∼7.0. Addition of $CaCO_3$ was modeled using MINTEQ to determine the post-remediation composition of the inflow chemistry (Table 2). This post-remediation chemistry results from pH-dependent precipitation of aluminum and iron(III) oxides and the sorption of various dissolved species to Fe(III) precipitates. Post-remediation chemistry of the inflow at 209 m was based on dissolved concentrations under the assumption that all precipitated and sorbed mass was removed within the treatment system. Under the first remediation plan, a closed system was assumed such that CO_2 degassing and Fe(II) oxidation did not occur. This plan is similar to treatment systems operated under anoxic conditions (*16*, *23*). Under the second remediation plan, an open system was assumed; CO_2 degassing was considered during $CaCO_3$ addition, and Fe(II) was oxidized and precipitated as Fe(III). This plan is very similar to the treatment system described by Maree et al. (*19*). OTEQ simulations of remediation plans were completed by replacing existing inflow chemistry at 209 m (reach 3) with post-remediation chemistry (Table 2).

Results

Existing Conditions. The geochemistry of the 3.5-km study reach is dominated by several key inflows. The inflow located at 209 m introduces acidic, metal-rich waters (Figure 2a−c,g−i) that act to dramatically decrease instream pH and increase metal concentrations (Figure 2d−f,j−l). Metal concentrations remain high and pH remains low for the next 640 m until the stream is buffered by the circumneutral waters of diverted Mineral Creek (850 m). A small decrease in pH occurs at ∼1160 m due to waters from the Carbon Lakes mining area, followed by increases in pH attributable to Porphyry and Big Horn Gulches (Figure 2a,d). With the exception of Pb, metal concentrations downstream of 850 m exhibit a gradual increase (1000−2000 m) followed by discrete decreases due to Porphyry and Big Horn Gulches (Figure 2e,f,j,k). Pb concentrations increase at ∼1800 m as the result of inflows at 1781 and 1941 (Figure 2i,l).

Simulations of pH, Fe(II+III), Al, Cu, As, and Pb reproduce the dominant features of the observed spatial profiles (Figure 2d−f,j−l). Simulations of Cd, Ni, and Zn also reproduce the observed spatial profiles and indicate that these components behave in a conservative manner under existing conditions. Notable discrepancies between simulated and observed conditions include the following: (i) overestimation of pH from 1200 to 2000 m and underestimation downstream of 2500 m (Figure 2d); (ii) overestimation of dissolved As from 350 to 850 m (Figure 2k); and (iii) failure to reproduce the gradual increase in total recoverable Al, As, Cu, and Fe(II+III) from 1000 to 2000 m (Figure 2e−f,j−k).

Remediation. Treatment of the inflow at 209 m results in similar spatial profiles of pH, dissolved Fe(II+III), dissolved Al, and dissolved Cu under both remediation plans (Figure 3a−d). Post-remediation pH is >6 throughout the study reach (Figure 3a), and concentrations of dissolved Fe, Al, and Cu are substantially reduced (Figure 3b−d). Dissolved Al concentrations are below the State of Colorado chronic standards (*34*) throughout the study reach (Figure 3c), whereas dissolved Cu concentrations remain above the hardness-dependent standard (Figure 3d). The effects of treatment on dissolved As and Pb concentrations differ under the two remediation plans with lower dissolved concentrations expected under the first remediation plan (Figure 3e,f). Dissolved Pb concentrations under the second remediation plan exceed dissolved concentrations under existing conditions downstream of 2400 m (Figure 3f). Post-remediation As concentrations are below the chronic standard, whereas post-remediation Pb concentrations remain above (Figure 3e,f).

Percent reductions (relative to existing conditions) in total recoverable Al and As concentrations at 3500 m are similar

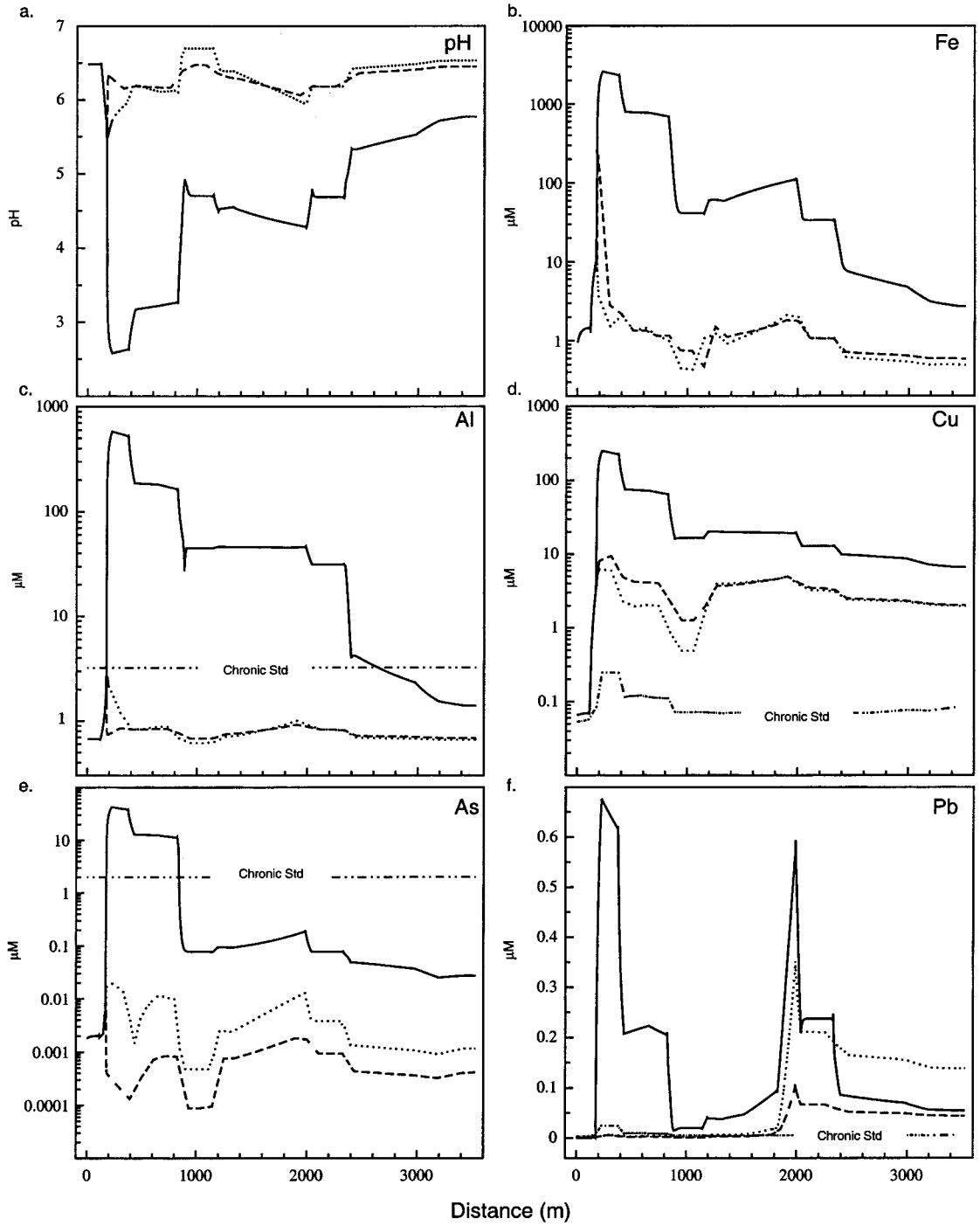

FIGURE 3. Simulated dissolved concentrations for existing conditions (solid line), remediation plan 1 (dashed line), and remediation plan 2 (dotted line). State of Colorado standards for chronic conditions are also shown (dash−dotted line).

under both remediation plans (Table 3). Reductions in total recoverable Cd, Cu, Fe(II+III), Ni, Pb, and Zn are higher under the second remediation plan than under the first. Percent reductions in dissolved Al, Cd, Cu, Fe(II+III), Ni, Zn, and H^+ are also higher under the second remediation plan (Table 3). In contrast, reductions in dissolved As and Pb are higher under the first remediation plan.

Discussion

Existing Conditions. Detailed characterization of existing conditions in the 3.5-km study reach was made possible by the combined tracer-dilution and synoptic sampling approach. This approach has the advantage of providing estimates of both streamflow and instream chemistry. Estimates of streamflow at 38 stream sites were calculated using sampled Br concentrations and the tracer-dilution method. Similar estimates of streamflow using conventional stream gaging techniques (*35*) would be difficult to obtain during the 6.3-h synoptic sampling period due to personnel requirements and problems associated with current meter measurements in shallow cobble-bed streams. Further, detailed sampling of observed inflows provides the data needed to reproduce in-stream metal concentrations. Component inflow concentrations for each reach were based on observed concentrations (Figure 2a−c,g−i; Table 1), and this assignment of inflow chemistry resulted in a good reproduction of observed stream data. One exception is the assignment of inflow concentrations for Pb, where Pb concentrations in

TABLE 3. Percent Decrease [Increase] in Stream Concentrations at 3500 m

	remediation plan 1		remediation plan 2	
component	total (%)	dissolved (%)	total (%)	dissolved (%)
pH (as H^+)		79.14		82.62
Al	62.89	50.90	62.89	52.82
As	84.85	98.38	84.86	95.45
Cd	0.29	0.35	1.53	1.53
Cu	48.06	69.65	66.53	70.35
Fe(II+III)	39.97	78.56	78.38	82.09
Ni	0.07	0.16	2.34	2.35
Pb	4.23	18.39	5.31	[152.28]
Zn	2.05	2.49	10.4	10.44

inflows at 1781 and 1941 m did not appear to be representative of Pb loading in reaches 14 and 15 (1530−1989 m; Figure 2i,l). Reassignment of Pb inflow concentrations was therefore necessary during the calibration process.

Precalibration results for the remaining metals were remarkably good considering the use of observed inflow data and default equilibrium constants. Simulation results for Al, As, Cu, and Fe(II+III) based on precalibration are generally similar to the calibrated results shown in Figure 2 at the scale presented. Closer examination of dissolved Fe(II+III) and As concentrations illustrates the need for calibration (Figure 2e,k insets). Better reproduction of dissolved Fe(II+III) concentrations was achieved by lowering the inflow pH in reaches 13−15 (1330−1989 m) and by decreasing ferrihydrite solubility (Figure 2e inset). The pH value used for reaches 13−15 (2.6) is similar to that of observed inflows in the upper part of the study reach (121, 209, and 297 m; Figure 2a). Although the calibrated solubility product (−5.29) differs from that used in previous model applications (*11*, *12*; ranging from −2.85 to −3.65), it is well within the reported range (*36*).

Reproduction of dissolved As concentrations was achieved by altering the surface complexation constant for H_2AsO_4 (Figure 2k inset); the value used is within the 99% confidence level reported by Dzombak and Morel (*31*) and is not surprising given the limited data on anion sorption to iron-(III) oxides (ref *31*, p 193). Despite this calibration, dissolved As concentrations from 350 to 850 m are not reproduced due to a lack of sorption sites (Fe(III) precipitates, Figure 2e). A final step in the calibration process was to replace the sampled inflow (Big Horn Gulch) in reach 18 (2331−2396 m) with the inflow at 2673 m to increase simulated pH downstream of 2330 m (Figure 2a,d). The need for this replacement suggests that the Big Horn Gulch sample was not representative of waters entering reach 18. The replacement inflow (2673 m) enters Mineral Creek from the same side of the stream as Big Horn Gulch and may be similar to subsurface waters entering reach 18 near the mouth of Big Horn Gulch. Further attempts to increase simulated pH downstream of 2330 m were not made so that simulations of remedial conditions would error on the conservative side; i.e., underestimation of pH results in underestimation of removal by sorption and prevents overly optimistic simulations of post-remediation water quality.

Final calibration results reproduce the general features of the observed spatial profiles in pH and metal concentration (Figure 2d−f,j−l), as well as several subtle features of the observed data. These subtle features include the sorption of Cu (Figure 2j inset) and the precipitation of Al (Figure 2f), two processes that become significant as inflows entering near Big Horn Gulch increase instream pH. Simulation of both processes was based on default equilibrium constants and did not require calibration. One feature of the observed data that is not reproduced by the simulations is the gradual increase in total recoverable Al, As, Cu, and Fe(II+III) from 1000 to 2000 m (Figure 2e,f,j−k). This section of Mineral Creek includes an abandoned mine dump upstream of Porphyry Gulch (Figure 1) and an acid−sulfate alteration zone. The failure of the simulations to reproduce this gradual increase suggests that unsampled inflows with high metal concentrations are entering the stream in reaches 11−15 (1194−1989 m). These high metal concentrations are consistent with the low-pH inflows used in reaches 13−15 (1330−1989 m) during model calibration. Adjustment of the inflow concentrations in reaches 11−15 was not included in the calibration process however (Table 1). A further complication is the uncertainty in streamflow estimates for reaches 13−15 due to the observed increase in Br concentrations. Additional study of this general area including sampling of subsurface flows may be warranted if actual remediation takes place.

Remediation. Simulation results indicate that both remediation plans would be expected to increase instream pH and decrease total recoverable metal concentrations along the 3.5-km study reach (Figure 3, Table 3). This analysis assumes negligible settling of freshly precipitated colloidal materials (precipitates and sorbed species) due to the rapidly flowing waters of Mineral Creek. Increased removal of total recoverable metals could likely be obtained by the construction of impoundments that increase the residence time for the aggregation and settling of colloidal material. With respect to dissolved concentrations, both plans result in concentrations that are either above (Cu, Pb) or below (Al, As) the State of Colorado chronic standards (Figure 3).

Although post-remediation conditions are generally similar under both remediation plans, some differences between the two plans are evident. The second remediation plan that includes the in-treatment oxidation of Fe(II) appears to be superior due to a higher removal of total recoverable metal concentrations and a lower $CaCO_3$ addition rate (Table 3). In addition, the second plan results in a higher reduction in dissolved concentrations for most metals (Al, Cd, Cu, Fe-(II+III), Ni, Zn, and H^+, Table 3). These higher removal percentages for total recoverable and dissolved concentrations are attributable to the oxidation of Fe(II) within the treatment system. This oxidation results in an increase in the amount of Fe(III) precipitation and a corresponding increase in the removal of other metals within the treatment system due to sorption.

In contrast, the first remediation plan is superior for the case of dissolved As and Pb (Table 3). This case arises due to different assumptions regarding Fe(II) in the two remediation plans. The first remediation plan represents a closed system in which the Fe(II) concentration in the 209 m inflow is unchanged by treatment (Table 2). Fe(II) is oxidized and precipitated as Fe(III) upon entering the stream subject to the specified Fe(II) percentages used to model photoreduction and oxidation (Table 1). Precipitated Fe(III) is therefore present in the water column downstream of the treatment system and is available for sorption of metals entering further downstream. The second remediation plan assumes complete oxidation of Fe(II) within the treatment system, resulting in a limited number of sorption sites within the water column downstream. The effect is especially striking for dissolved Pb due to sources below 1530 m. The lack of precipitated Fe(III) under the second remediation plan results in an increase in dissolved Pb over existing conditions. This comparison of remediation plans illustrates the importance of colloidal Fe(III) in sorbing metals as noted by Paulson and Balistrieri (*37*), a factor that should be considered in treatment system design. For the present case, the effects of the two remediation plans on dissolved Pb may be less important downstream of the study reach, where other sources of Fe provide additional sorptive capacity.

Reactive Transport Modeling. Although the hypothetical remediation plans presented above are gross simplifications of complex treatment systems, the modeling analysis demonstrates the utility of reactive transport modeling to estimate post-remediation water quality. Consideration of more complex treatment systems and treatment plans involving multiple inflows is easily accomplished within the framework of the reactive transport model. The process-based approach implemented within OTEQ has two advantages when considering the effects of acid mine drainage and treatment plant design. First, use of a chemical equilibrium submodel allows for the consideration of the solute (component) interaction that occurs in aquatic systems. In particular, interactions between pH and metal oxide precipitation are explicitly considered (*11*, *12*). Furthermore, the sorption process is directly tied to the precipitation of iron(III) oxides, as sorbent mass is based on the concentration of Fe(III) precipitates (*10*). Use of the simulated Fe(III) precipitate concentration eliminates the need to specify sorbent mass, thereby simplifying the calibration process. Second, the process-based approach is transferable; mass action equations within the equilibrium submodel are valid over a range of pH such that the model is applicable to both pre- and post-remediation conditions. Most models based on first-order rate constants do not share this characteristic; rate constants developed under existing conditions may not be appropriate for the elevated pH conditions and decreased metal concentrations associated with remediation.

Although the approach presented here is a promising tool for analysis of treatment options, several limitations should be kept in mind. First, the analysis relies on field data that provide an accurate and detailed description of streamflow, inflow chemistry, and in-stream water quality. Implementation of the tracer-dilution method and detailed spatial sampling requires a considerable investment in personnel, equipment, and laboratory analysis. Simulation efforts based on limited data may be fraught with uncertainty and of little use for treatment plant design. Second, sampled inflow chemistry within the 3.5-km study reach is generally representative of the inflow loading that actually occurs. This fortuitous situation is often not the case in the acid mine drainage streams studied by the authors. The inflows most frequently sampled are surface inflows (springs and tributaries) that may not necessarily represent average inflow chemistry for a given reach. This situation requires expert judgment or sampling of subsurface flows to determine the groundwater contribution. Inflow assignment based on expert judgment is complicated by the fact that inflow concentrations of reactive solutes may not be determined from simple mass balance, while sampling of subsurface flows may increase study costs. Third, the subject study was conducted in the early fall and is thought to be representative of low-flow conditions. Additional studies under other flow regimes (e.g., high flow) may be necessary to bracket the behavior of the geochemical system. Fourth, although the approach is more transferable than the rate-constant approach, differences between existing and post-remediation chemistry complicate model application. For example, Bigham et al. (*38*) describe the dependence of iron(III) oxide precipitation on ambient pH. Solid phases formed at low pH (e.g., existing conditions) may differ from phases forming at higher pH (post-remediation), such that the calibrated model may not be representative of post-remediation conditions. The sorptive properties of the solid phases may also differ; sorption onto iron(III) oxides explained the behavior of As, Cu, and Pb for the pH regime considered here, whereas sorption onto aluminum and manganese oxides may play a role at post-remediation pH. Furthermore, some metals may not be subject to sorption reactions under existing conditions (e.g., Zn in the work presented here) but are likely to sorb at the higher pH levels associated with remediation. This situation prevents calibration of sorption parameters as illustrated here for As. Despite these caveats, the model's ability to simulate pH, metal oxide precipitation−dissolution, and pH-dependent sorption provides a means of evaluating the complex interactions that are likely to occur in acid mine drainage streams subject to remediation.

Acknowledgments

Funding for this work was provided by the U.S. Geological Survey's Toxic Substances Hydrology Program. Field and laboratory assistance was provided by Larry Schemel, Marisa Cox, Linda Gerner, Suzanne Paschke, Phil Verplanck, Katie Walton-Day, Jon Evans, Ken Leib, Douglas Burkhardt, Bruce Stover, Anna Day, and Brad Smith. Figure 1 was created using a base map provided by Carl Rich and Richard Pelltier. The authors appreciate the helpful comments provided by Bob Broshears and Chuck Cravotta.

Supporting Information Available

Chemical data from the stream and inflow samples. This material is available free of charge via the Internet at http://pubs.acs.org.

Literature Cited

(1) Bencala, K. E.; Walters, R. A. *Water Resour. Res.* **1983**, *19*, 718−724.
(2) Bencala, K. E. *Water Resour. Res.* **1983**, *19*, 732−738.
(3) Kuwabara, J. S.; LeLand, H. V.; Bencala, K. E. *J. Environ. Eng.* **1984**, *110*, 646−655.
(4) Kimball, B. A.; Broshears, R. E.; Bencala, K. E.; McKnight, D. M. *Environ. Sci. Technol.* **1994**, *28*, 2065−2073.
(5) Choi, J.; Hulseapple, S. M.; Conklin, M. H.; Harvey, J. W. *J. Hydrology* **1998**, *209*, 297−310.
(6) Harvey, J. W.; Fuller, C. C. *Water Resour. Res.* **1998**, *34*, 623−636.
(7) Runkel, R. L. *Water Resour. Invest.* (*U.S. Geol. Surv.*) **1998**, *No.* 98-*4018*, 73 (http://co.water.usgs.gov/otis).
(8) Worman, A.; Forsman, J.; Johansson, H. *J. Environ. Eng.* **1998**, *124*, 122−130.
(9) Runkel, R. L.; Bencala, K. E.; Broshears, R. E.; Chapra, S. C. *Water Resour. Res.* **1996**, *32*, 409−418.
(10) Runkel, R. L.; Kimball, B. A.; McKnight, D. M.; Bencala, K. E. *Water Resour. Res.* **1999**, *35*, 3829−3840.
(11) Broshears, R. E.; Runkel, R. L.; Kimball, B. A.; McKnight, D. M.; Bencala, K. E. *Environ. Sci. Technol.* **1996**, *30*, 3016−3024.
(12) Runkel, R. L.; McKnight, D. M.; Bencala, K. E.; Chapra, S. C. *Water Resour. Res.* **1996**, *32*, 419−430.
(13) Achterberg, E. P.; Braungardt, C.; Morley, N. H.; Elbaz-Poulichet, F.; Leblanc, M. *Water Res.* **1999**, *33*, 3387−3394.
(14) Benner, S. G.; Blowes, D. W.; Gould, W. D.; Herbert, R. B.; Ptacek, C. J. *Environ. Sci. Technol.* **1999**, *33*, 2793−2799.
(15) Cravotta, C. A.; Trahan, M. K. *Appl. Geochem.* **1999**, *14*, 581−606.
(16) Drury, W. J. *Water Environ. Res.* **1999**, *71*, 1244−1250.
(17) Erten-Unal, M.; Wixson, B. G. *Water Air Soil Pollut.* **1999**, *116*, 501−522.
(18) Hamilton, Q. U. I.; Lamb, H. M.; Hallett, C.; Proctor, J. A. *J. CIWEM* **1999**, *13*, 93−103.
(19) Maree, J. P.; Strydom, W. F.; de Beer, M. *Water Sci. Technol.* **1999**, *39*, 231−238.
(20) Shokes, T. E.; Moller, G. *Environ. Sci. Technol.* **1999**, *33*, 282−287.
(21) Chang, I. S.; Shin, P. K.; Kim, B. H. *Water Res.* **2000**, *34*, 1269−1277.
(22) McKinnon, W.; Choung, J. W.; Xu, Z.; Finch, J. A. *Environ. Sci. Technol.* **2000**, *34*, 2576−2581.
(23) Nuttall, C. A.; Younger, P. L. *Water Res.* **2000**, *34*, 1262−1268.
(24) Kimball, B. A.; Bencala, K. E.; Besser, J. M. *Water Resour. Invest.* (*U.S. Geol. Surv.*) **1999**, *No.* 99-*4018A*, 3−7.
(25) Bencala, K. E.; McKnight, D. M. In *Chemical Quality of Water and the Hydrologic Cycle*; Averett, R. C., McKnight, D. M., Eds.; Lewis Publishers: Ann Arbor, MI, 1987; pp 255−269.
(26) Kimball, B. A.; Runkel, R. L.; Walton-Day, K.; Bencala, K. E. *Appl. Geochem.* (in press).
(27) Kilpatrick, F. A.; Cobb, E. D. *Techniques of Water-Resources Investigations* (*U.S. Geological Survey*) Book 3, Chapter A16; U.S. Geological Survey: Reston, VA, DC, 1985; p 52.

(28) To, T. B.; Nordstrom, D. K.; Cunningham, K. M.; Ball, J. W.; McCleskey, R. B. *Environ. Sci. Technol.* **1999**, *33*, 807−813.
(29) Brown, E.; Skougstad, M. W.; Fishman, M. J. *Techniques of Water-Resources Investigations* (*U.S. Geological Survey*) Book 5 Chapter A1; U.S. Geological Survey: Reston, VA, 1970; p 103.
(30) Allison, J. D.; Brown, D. S.; Novo-Gradac, K. J. Report EPA/600/3-91/021. U.S. EPA: Washington, DC, 1991; p 106.
(31) Dzombak, D. A.; Morel, F. M. M. *Surface Complexation Modeling: Hydrous Ferric Oxide;* John Wiley and Sons: New York, 1990; p 393.
(32) McKnight, D. M.; Kimball, B. A.; Bencala, K. E. *Science* **1988**, *240*, 637−640.
(33) Nordstrom, D. K. *U.S. Geol. Surv. Water-Supply Pap.* **1985**, *No. 2270*, 113−119.
(34) Colorado Department of Public Health and Environment. *The Basic Standards and Methodologies for Surface Water, Regulation No. 31* (*5 CCR 1002-31*); State of Colorado: Denver, 2000; p 58 (http://www.cdphe.state.co.us/regs/100231u.pdf).
(35) Rantz, S. E.; et al. *U.S. Geol. Surv. Water-Supply Pap.* **1982**, *No. 2175*, 284.
(36) Langmuir, D.; Whittemore, D. O. *Adv. Chem. Ser.* **1971**, *106*, 209−234.
(37) Paulson, A. J.; Balistrieri, L. *Environ. Sci. Technol.* **1999**, *33*, 3850−3856.
(38) Bigham, J. M.; Schwertmann, U.; Pfab, G. *Appl. Geochem.* **1996**, *11*, 845−849.

Received for review May 16, 2001. Revised manuscript received December 3, 2001. Accepted December 10, 2001.

ES0109794